Clays and Clay Minerals, Vol. 57, No. 3, 302–310, 2009.

APPLICATION OF ^{29}Si AND ^{27}Al MAS NMR SPECTROSCOPY TO THE STUDY OF THE REACTION MECHANISM OF KAOLINITE TO ILLITE/MUSCOVITE

MARCO MANTOVANI[1], ALBERTO ESCUDERO[2], AND ANA ISABEL BECERRO[1,*]

[1] Instituto de Ciencia de Materiales de Sevilla – Dpto. de Química Inorgánica, CSIC-US, c/ Américo Vespucio, 49, 41092 Sevilla, Spain

[2] Bayerisches Geoinstitut, Universität Bayreuth. Bayreuth, Germany

Abstract—Understanding the mechanisms for illitization of clay minerals has important applications in reconstructing geologic histories and determining the origins of physical and chemical characteristics of buried sediments. While many studies have been carried out on this topic, few have focused on the mechanism of illite formation from kaolinite. The purpose of this study was to investigate more deeply the illitization of kaolinite in KOH solution at a high solid/liquid ratio (1000 mg/mL). X-ray diffraction (XRD) and infrared spectroscopy were used to follow the formation of new crystalline phases and the composition of the octahedral sheet, while the transformation of the Si and Al local environments was analyzed by ^{29}Si and ^{27}Al magic angle spinning nuclear magnetic resonance spectroscopy (MAS NMR). The results revealed that the first reaction stage consists of the diffusion of Al from the octahedral to the tetrahedral sheet of the kaolinite TO layers, giving rise to the precursors of the illite/muscovite nuclei. Combination of XRD with ^{27}Al MAS NMR measurements indicated that a minimum amount of tetrahedral Al is required in the original TO layer before condensation of a second tetrahedral sheet occurs to complete the formation of the illite/muscovite TOT layers.

Key Words—Al-27 MAS NMR, Hydrothermal Experiments, Illite, IR Spectroscopy, Kaolinite, Muscovite, Si-29 MAS NMR, X-ray Diffraction.

INTRODUCTION

The degree of reaction of clay minerals to form illite is frequently used as a geothermometer to allow reconstructions of the thermal and tectonic history of sedimentary basins (Weaver and Beck, 1971; Schoonmaker *et al*., 1986), and of active and fossil hydrothermal systems (Inoue and Utada, 1983; Jennings and Thompson, 1986). The chemical consequences of this reaction may influence the development of geopressures, growth faults, oil migrations, mineral cements, and porosity.

Specifically, the reaction mechanisms for illitization of smectite have been classified into three broad categories: solid-state transformation (SST), dissolution crystallization (DC), and Ostwald ripening (OR) (Altaner and Ylagan, 1997). Considerable controversy exists as to which reaction mechanism applies to illitization in natural systems (Ahn and Buseck, 1986; Inoue *et al*., 1990; Yau *et al*., 1987; Inoue *et al.*, 1988; Altaner and Ylagan, 1997). For example, studies of smectite illitization in burial diagenetic or hydrothermal systems may implicitly assume that illitic illite-smectite (I-S) forms from a smectitic precursor. Illite and I-S can form readily from a kaolinite precursor, however. In fact, studies of the paragenesis of authigenic illite in arkosic sandstones of various ages and from various regions have revealed that the illitization of kaolinite is an important reaction accounting for the formation of authigenic illite in sandstones during burial diagenesis (Hancock and Taylor, 1978; Sommer, 1978; Dutta and Suttner, 1986; Martín-Martín *et al*., 2006). Direct precipitation of illitic minerals from a kaolin precursor has also been described in shallow-buried sandstone units from the Norwegian Continental Shelf (De Almeida Martins, 1999).

Velde (1965) synthesized muscovite from kaolinite and KOH solutions, and much experimental illitization of kaolinite in aqueous solutions containing K has followed in the years since. Most of the studies report results on the kinetics of kaolinite illitization (Chermak and Rimstidt, 1990; Huang, 1993; Bauer *et al*., 1998; Bauer and Berger, 1998), whereas papers which deal with the kaolinite-to-illite reaction mechanism are very scarce. A series of interesting studies on this subject has been carried out by Bentabol and co-workers (Bentabol *et al*., 2003a, 2003b, 2006) using temperatures of 200 and 300ºC and small solid/liquid ratio values (from 60 to 250 mg/mL), which favor a DC mechanism; those authors use XRD and transmission electron microscopy (TEM) to determine the structural and chemical characteristics of the reaction products.

In order to obtain a more complete overview of the illitization of kaolinite at different solid/liquid ratios, a set of experiments was performed in the present study using a much larger solid/liquid ratio (1000 mg/mL) than that used in the studies described above. Special

* E-mail address of corresponding author:
anieto@icmse.csic.es
DOI: 10.1346/CCMN.2009.0570303

emphasis was placed on the first reaction stages, when incipient illite/muscovite nuclei (in the pure $K_2O/Al_2O_3/SiO_2/H_2O$ system, as is the present case, muscovite and illite are indistinguishable and are grouped as muscovite/illite – Bailey, 1984) are being formed from kaolinite layers. Hydrothermal treatment, at 500 bars external pressure, of a powdered kaolinite with a KOH solution, which serves as the K source, for varying periods of time is, essentially, the methodology followed. Transformation of the Si and Al environments was followed by ^{29}Si and ^{27}Al MAS NMR spectroscopy, which allow detection and study of the illite/muscovite nuclei formed at the first reaction stages, when the XRD patterns only show kaolinite reflections.

EXPERIMENTAL

Hydrothermal experiments

100 mg of KGa-2 kaolinite powder obtained from the Source Clays Repository (of The Clay Minerals Society, and based at Purdue University, West Lafayette, Indiana, USA) with the chemical formula $(Ca_{tr}K_{tr})(Si_{4.00})^{IV}(Al_{3.66}Fe_{0.07}Ti_{0.16}Mn_{tr}Mg_{tr})^{VI}O_{10}(OH)_8$ (Mermut and Faz Cano, 2001), was submitted to hydrothermal treatment in gold capsules with 100 μL of 2.58 M KOH solution for 1, 4, 7, 13, and 24 h at 500 bars external pressure and 300ºC. The experiments were carried out at the Hydrothermal Laboratory at the Bayerisches Geoinstitut (Bayreuth, Germany). The product from the reaction was a slightly moistened powder, where separation of the liquid and solid phases was not possible due to the high solid/liquid ratio employed. For this reason, the present study does not report on the liquid product composition, as other, related studies do. The reaction products were washed several times with distilled water by filtration and dried at 40ºC.

Characterization techniques

X-ray powder diffraction (XRD) patterns were obtained using a Siemens D-501 diffractometer, with Ni-filtered CuKα radiation, steps of 0.05º, and a counting time of 3 s.

Fourier transform infrared spectroscopy (FTIR) was performed using a Nicolet 510 FTIR instrument equipped with a DTGS detector. Spectra were recorded in the 1400–400 cm^{-1} range with a resolution of 2 cm^{-1}. The measurements were taken using dried KBr pellets, which were prepared by mixing and pressing 1.5 mg of sample with 100 mg of KBr.

^{29}Si Magic Angle Spinning Nuclear Magnetic Resonance (MAS-NMR) spectroscopy measurements were carried out using a Bruker DRX400 (9.39 T) spectrometer equipped with a multinuclear probe, with 4 mm zirconia rotors spinning at 10 kHz. A single pulse sequence was used, with a pulse length of 2.5 μs (π/2 pulse length = 7.5 μs), an observation frequency for ^{29}Si of 79.49 MHz, and an optimized delay time of 15 s. The chemical shifts are reported in ppm from Tetramethylsilane (TMS). ^{27}Al MAS-NMR spectra were recorded at 104.26 MHz with a pulse length of 1.1 μs (π/2 pulse length = 11 μs) and a delay time of 0.5 s. The chemical shifts are reported in ppm relative to a 0.1 M $AlCl_3$ solution.

RESULTS

The XRD pattern of kaolinite (Figure 1, upper) consists of two types of reflections, basal (symmetric lines, 00*l*) and general (asymmetric lines, *hk*). The position of the 001 reflection indicates a basal spacing (*c* unit-cell parameter) of 7.16 Å corresponding to the size of one tetrahedral and one octahedral sheet forming the kaolinite layers (TO layers). A clear preferential orientation of the platy crystals occurred in the sample, as inferred from the enhancement of the 00l (at 12.4º2θ) and the 002 (at 24.9º2θ) reflections. On the other hand, the d_{060} value (one sixth of the *b* unit-cell parameter) is 1.49 Å (=62.3º2θ), in good agreement with the pure dioctahedral nature of the sample (Grim, 1968). Finally, the XRD pattern showed the characteristic indications of *b*-axis disorder of the KGa-2 kaolinite sample, with diffusion of the 020 reflection (20º2θ).

The XRD patterns of the samples treated for 1, 4, and 7 h (Figure 1) showed only unmodified reflections of kaolinite, as well as an extra reflection at ~30º2θ. The patterns of the samples treated for 13 and 24 h (Figure 1) revealed, in addition to the characteristic kaolinite reflections, a set of new reflections that indicate the crystallization of illite/muscovite, more pronounced in the sample treated for 24 h. The positions of the illite/muscovite basal reflections indicate a basal spacing of 10.2 Å, characteristic of TOT layers with dehydrated interlayer K^+ ions. The location of the 060 reflection corresponds to a d_{060} value of 1.50 Å, slightly higher than that of the parent kaolinite. The reflections corresponding to kaolinite were unchanged throughout the process, as observed, for example, in the positions of the 001 and 060 reflections (marked with dotted lines in Figure 1).

Infrared (IR) spectra of the kaolinite before and after the hydrothermal treatment for 1, 4, 7, 13, and 24 h are reported in Figure 2. The IR spectrum of a sample of kaolinite treated for 24 h at a much greater pressure (3500 bars), which shows almost complete transformation in illite/muscovite, is included at the bottom of the figure for comparison purposes. The starting sample produced bands characteristic of kaolinite KGa-2, as given in table 1 of Madejová and Komadel (2001); all were assigned to Si-O stretching modes and Al-O-Si and Si-O-Si deformation modes. The presence of a very low-intensity band at ~ 855 cm^{-1} (marked with an asterisk) could be due to the small amount of Fe present in the octahedral sheet of the kaolinite (see the chemical

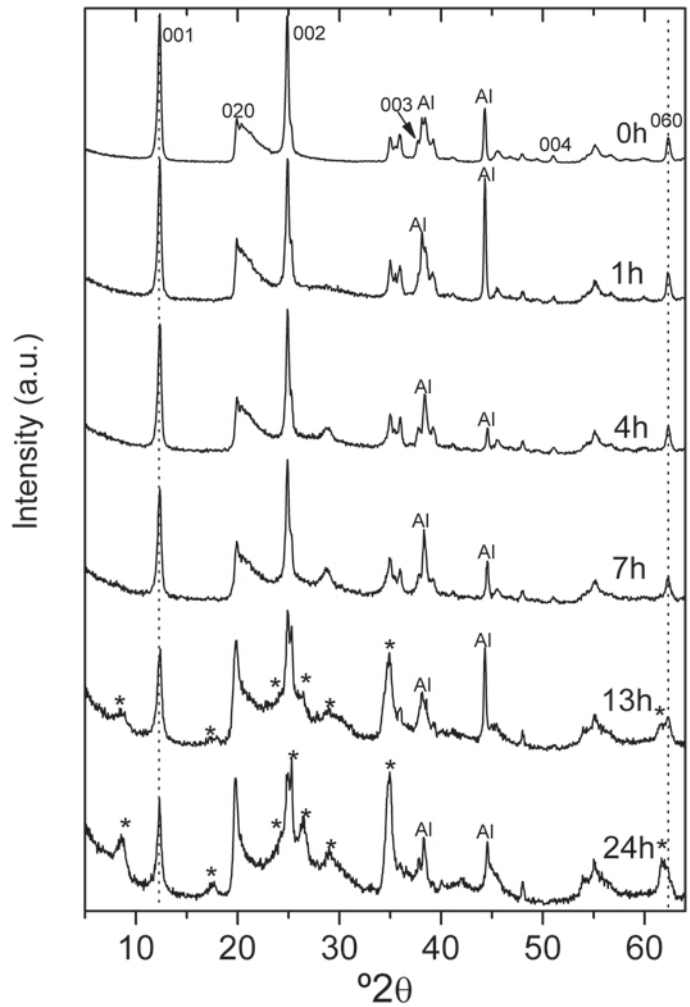

Figure 1. XRD patterns of kaolinite before and after hydrothermal treatment in KOH solution at increasing reaction times. The dotted lines show the constant 2θ position of the 001 and 060 kaolinite reflections. *: Reflections from muscovite/illite. Al: aluminum peaks from the sample holder.

formula in the Experimental section). Identical spectra were registered for the samples treated for 1, 4, and 7 h while samples treated for 13 and 24 h showed a decrease in the intensity of the bands at 1104, 914, and 754 cm^{-1} and a loss of resolution of the bands at 1033 and 1008 cm^{-1}; these are clear signs of the transformation to illite/muscovite, as observed in the illite/muscovite spectrum at the bottom of Figure 2. The band assigned to the presence of octahedral Fe in the starting kaolinite shifted toward greater wavenumbers (~875 cm^{-1}), characteristic of AlFeOH deformation modes in TOT silicates (Madejová and Komadel, 2001). Some Fe is, therefore, making up part of the octahedral sheet of the newly formed illite/muscovite phase.

The ^{29}Si MAS NMR spectrum of the starting kaolinite (Figure 3, upper) contained a single, symmetric ^{29}Si resonance at −91.26 ppm (Kinsey *et al*., 1985), corresponding to the unique Si environment in the sample, consisting of Si atoms surrounded by three SiO_4 tetrahedra $-Q^3(0Al)-$ (nomenclature from Liebau, 1985), in good agreement with the chemical formula of the KGa-2 kaolinite sample (see the Experimental section). The position of this signal does not change with the treatment, although an increase in the FWHM value was observed with reaction time (Figure 3), indicating a progressive disorder in the local environment of the Si nuclei of the remnant kaolinite particles.

As reaction progressed, a new broad contribution developed on the high-frequency side of the main resonance, which was appreciable after only 1 h of treatment and the intensity of which increased with increasing reaction time. The new band is located in the ppm range characteristic of $Q^3(1Al)$, $Q^3(2Al)$, and $Q^3(3Al)$ environments (Weiss *et al*., 1987). The low resolution of the signal fails to provide reliable results in terms of the percentage of each environment.

The ^{27}Al MAS NMR spectrum of the starting kaolinite (Figure 4, upper) consisted of a signal at

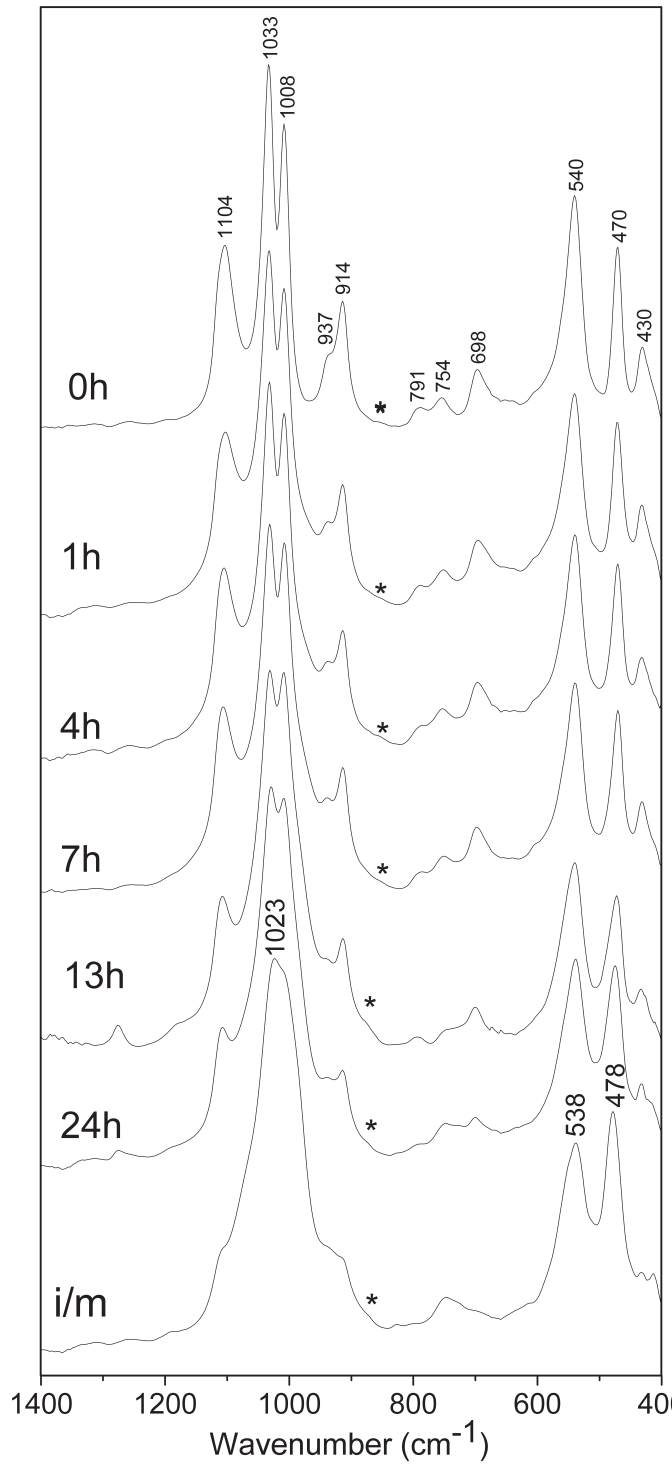

Figure 2. IR spectra of kaolinite before and after hydrothermal treatment in KOH solution at increasing reaction times. The lowermost spectrum corresponds to a kaolinite sample treated at high pressure, which transforms it to illite/muscovite. * indicates the position of a band due to the presence of Fe in the octahedral sheet of the kaolinite and illite/muscovite.

1.1 ppm, corresponding to Al in the octahedral sheet of the clay (Kinsey *et al*., 1985; Woessner, 1989). When the sample was submitted to hydrothermal treatment for 1 h (Figure 4), a new signal was clearly observed at 60.0 ppm, which progressively decreased in intensity with increasing reaction time, giving rise to a second

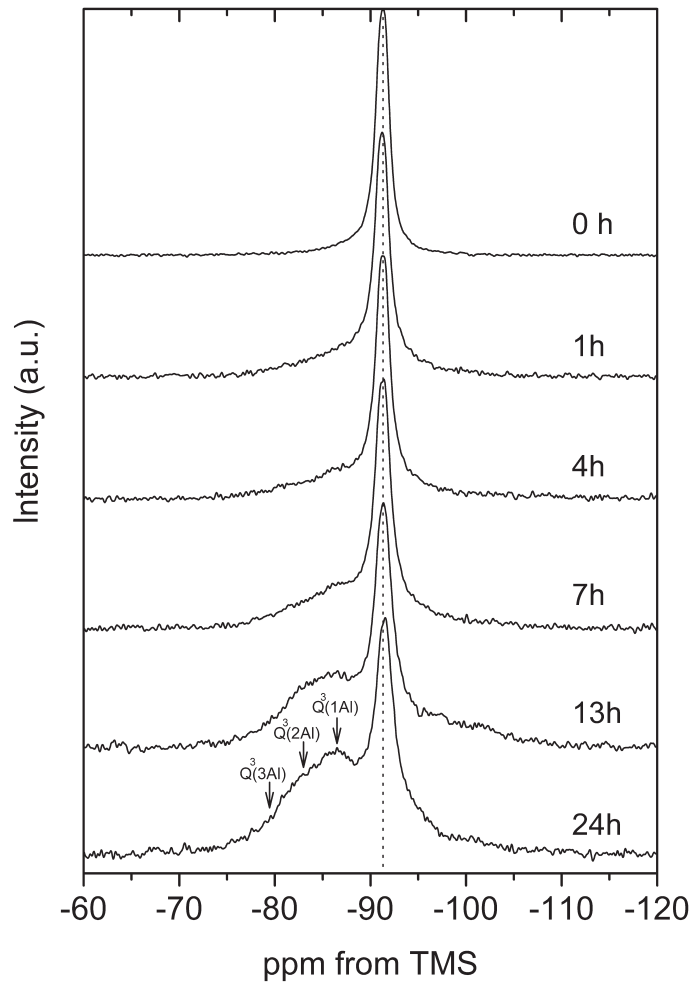

Figure 3. ^{29}Si MAS NMR spectra of kaolinite before and after hydrothermal treatment in KOH solution at increasing reaction times. The dotted line indicates the constant-frequency value of the main signal. The positions expected for the different $Q^3(1-3Al)$ in muscovite/illite are marked with arrows.

signal at 68.8 ppm. Both signals coexisted with the resonance at 1.1 ppm in all samples. The signals at 60.0 and 68.8 ppm are both in the frequency range characteristic of tetrahedral Al, denoting, therefore, that a partial change in the coordination polyhedron of Al was produced as a consequence of the treatment, the reaction products containing Al in both octahedral and tetrahedral coordination.

DISCUSSION

A schematic representation showing the chemical and structural differences between kaolinite and illite/muscovite structures (Figure 5) illustrates that kaolinite layers (TO) are made up of a sheet of [SiO_4] tetrahedra and a sheet of edge-sharing [AlO_6] octahedra, charge balanced, with only weak bonds holding successive layers together in the stack. On the other hand, illite layers (TOT) are made up of one octahedral sheet sandwiched between two tetrahedral sheets. Isomorphic substitutions take place in both sheets, creating a negative layer charge that is balanced by interlayer K^+. In the pure $K_2O/Al_2O_3/SiO_2/H_2O$ system, as is this case, substitution takes place only in the tetrahedral sheet, where some Al^{3+} substitutes for Si^{4+}. In view of these differences, transformation of kaolinite to illite/muscovite implies the substitution of some of the Si^{4+} in the tetrahedral sheet of kaolinite by Al^{3+}; condensation of a second tetrahedral sheet, and the introduction of K^+ into the interlayer space in order to satisfy the charge deficiency developed as a consequence of such substitution.

Bentabol *et al*. (2003a, 2003b, 2006), in their study of illitic phases formed from kaolinite in hydrothermal conditions using small solid/liquid ratios, observed two contrasting mechanisms of illitization: (1) the direct precipitation from solution, in which illitic phases are formed from zeolites and feldspathoid phases precipitated after the dissolution of kaolinite in NaOH + KOH solutions (high-pH conditions); and (2) the formation of illitic phases directly from kaolinite by topotactic

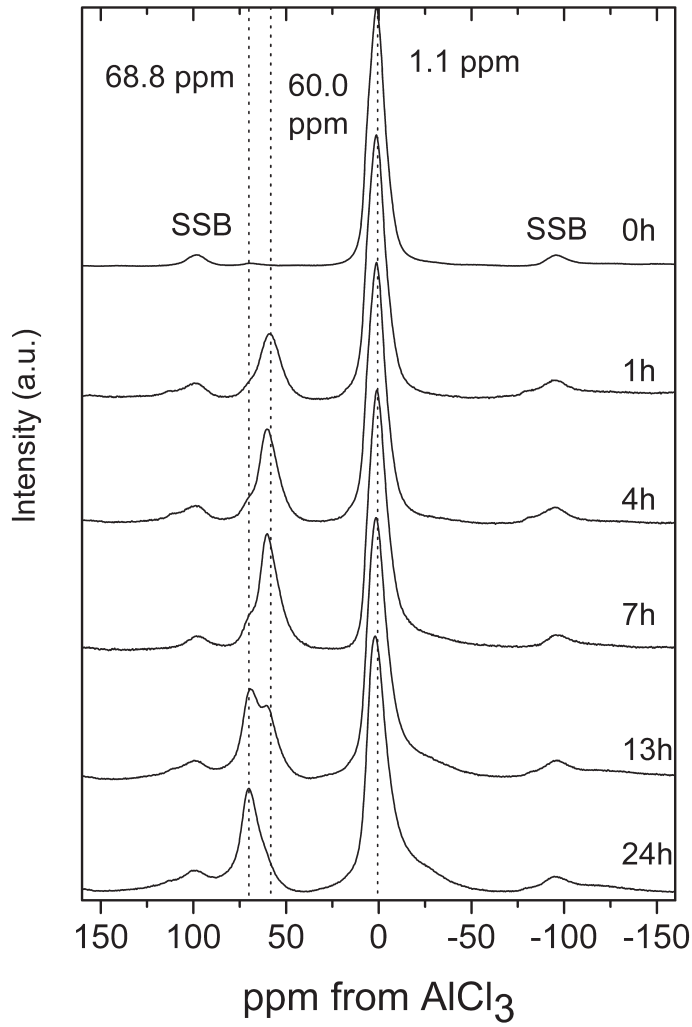

Figure 4. ^{27}Al MAS NMR spectra of kaolinite before and after hydrothermal treatment in KOH solution at increasing reaction times. The low-intensity signals at 98.2 ppm and 95.7 ppm are spinning side bands (SSB) of the Al resonance at 1.1 ppm.

replacement. The latter mechanism is favored by the addition of $MgCl_2$ to the NaOH + KOH solution, which reduces the pH and avoids the kaolinite dissolution. The results of the present work indicate that illitization of kaolinite in high-pH solutions using large solid/liquid ratios takes place through a topotactic replacement, where kaolinite layers progressively transform to illite layers without dissolution of the kaolinite crystals.

The XRD patterns in Figure 1 indicate that illite/muscovite crystals with domain size large enough to be detected by diffraction were formed after only 13 h of reaction. At shorter reaction times, the XRD patterns show only reflections of kaolinite, with position and intensity identical to those of the starting material. Similar conclusions were reached from the IR spectra. This is not the case, however, for the ^{29}Si and ^{27}Al MAS NMR spectra, which revealed appreciable changes even after only 1 h of reaction. A broad, new contribution to the ^{29}Si MAS NMR spectra (Figure 3) was observed on the high-frequency side of the main kaolinite resonance, the intensity of which increased with increasing reaction time and the position of which coincided with that of the $Q^3(1Al)$, $Q^3(2Al)$, and $Q^3(3Al)$ environments

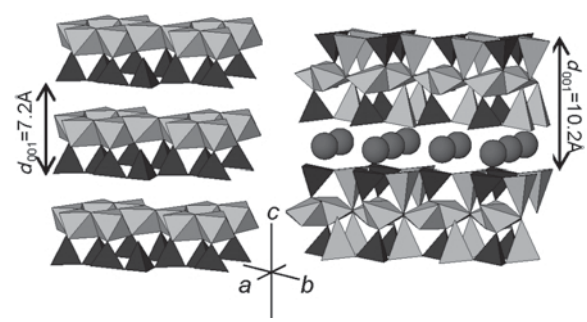

Figure 5. Schematic representation of the kaolinite (left) and illite/muscovite (right) structure. Light gray polyhedra – Al; dark gray tetrahedra – Si; spheres – K.

(Engelhardt and Michel, 1987). Therefore, after only 1 h of reaction, signs emerged of the presence of Al in the tetrahedral sheet of some kaolinite layers.

The assignment of the new signals observed in the ^{27}Al MAS NMR spectra (Figure 4) at 60.0 and 68.8 ppm is not straightforward. Tetrahedral Al in pure muscovite resonates at 70 ppm (Sanz and Serratosa, 1984); the high-frequency ^{27}Al NMR resonance (at 68.8 ppm) in the spectra of the samples treated for 13 and 24 h can, therefore, be assigned to Al in the tetrahedral sheet of the illite/muscovite phase formed as a consequence of the reaction. However, the assignment of the resonance at 60 ppm observed in the spectra of all treated samples is not that simple. The signal is in the frequency range characteristic of Q^4 Al environments in feldspars (55−68 ppm) (Kirkpatrick *et al*., 1985); the presence of feldspar nuclei in the sample would imply, however, the existence of Q^4 Si environments producing ^{29}Si NMR signals in the −95 to −100 ppm frequency range. The possible presence of feldspars as the cause of the ^{27}Al NMR signal at 60.0 ppm can be discarded because no ^{29}Si signal in the frequency range characteristic of feldspars was observed in any of the spectra of the samples that showed the greatest intensity for that ^{27}Al signal (samples treated for 1, 4, and 7 h). An alternative explanation is obtained from the observed tendency for deshielding at tetrahedrally coordinated Al with increasing substitution of Al for Si in the tetrahedral sheet of layered aluminosilicates (Kinsey *et al*. 1985), *i.e.* the tetrahedral ^{27}Al signal shifts toward higher-frequency values as the amount of Al nuclei in the tetrahedral sheet of the structure increases. The hydrothermal treatment of kaolinite must induce a diffusion of Al from the octahedral to the tetrahedral sheet of the layers, as indicated by the Si signals corresponding to $Q^3(n\text{Al})$ environments. Such diffusion was also observed by Pollard (1971) in his study of smectite illitization, in which Al and Si diffuse through the hydrous interlayer and the tetrahedral sheet distorts while Al replaces Si. Thus, at short reaction times, the amount of Al that has diffused from the octahedral to the tetrahedral sheet of the kaolinite sample is expected to be small, and those tetrahedral Al nuclei produce the signal at 60.0 ppm observed in the ^{27}Al NMR spectra of the samples treated during short periods of times (1, 4, and 7 h). With increased reaction time, the amount of Al in the tetrahedral sheet increases and the ^{27}Al NMR signal shifts toward higher-frequency values. Unfortunately, the fact that ^{27}Al is a quadrupolar nucleus hinders a quantitative analysis of the ^{27}Al NMR spectra to confirm this assignment (Sanz and Serratosa, 1984; Lipsicas *et al*., 1984; Kinsey *et al*., 1985). An observation supporting this hypothesis was obtained, however, from the ^{29}Si NMR signals, which shift toward higher-frequency values as the number of Al neighbors increases in layered silicates (Engelhardt and Michel, 1987). The approximate positions of the individual contributions expected for the three different Si environments – Q^3(1Al), Q^3(2Al), and Q^3(3Al) – are marked with arrows in Figure 3. The intensity observed in the Q^3(2Al) and Q^3(3Al) region is clearly greater in the case of the samples treated for longer periods, which agrees with the assignment made above for the ^{27}Al MAS NMR peaks.

The first stage in the illitization of kaolinite in the conditions of the present experiments is the diffusion of Al from the octahedral to the tetrahedral sheet of the kaolinite layers, as indicated by these observations. The Al diffusion gives rise to partially transformed kaolinite layers which must be the precursors of the illite/muscovite nuclei. In order to go from a TO layer, characteristic of kaolinite, to a TOT layer, typical of the illite/muscovite structure, a second tetrahedral sheet must be connected to the pre-existing TO layer. The XRD patterns only show a 10.2 Å peak characteristic of TOT illite/muscovite layers after 13 h of treatment. At that reaction time, the ^{27}Al MAS NMR spectrum exhibits a change in the intensity ratio of the 68.8 ppm/60.0 ppm signals. That condensation of a second tetrahedral sheet seems to indicate that a minimum amount of tetrahedral Al must be produced.

Extent of the reaction

The diffusion of Al from the octahedral to the tetrahedral sheet of kaolinite at the first reaction stages implies: (1) the formation of vacancies in the octahedral sheet; (2) the displacement of Si atoms from the tetrahedral sheet due to the incoming Al atoms; and (3) the creation of a negative layer charge as a consequence of the replacement of Si^{4+} by Al^{3+} in the tetrahedral sheet, which will be compensated by interlayer K^+ taken from the KOH fluid phase.

The increasing number of vacancies created in the octahedral sheet of the kaolinite layers due to the Al diffusion implies a decrease in the *b* unit-cell dimension of the kaolinite structure with increasing reaction time. Likewise, the introduction of K^+ ions in the interlayer space of these transforming layers should be reflected by a slight increase in the *c* unit-cell dimension of the kaolinite structure. None of these conditions was observed in the XRD patterns of Figure 1, where both the 001 (*c* unit-cell parameter) and the 060 (1/6 of the *b* unit-cell parameter) kaolinite reflections remained at the same 2θ position for any reaction time. Furthermore, the ^{29}Si NMR spectra of all reacted samples exhibited a main signal at exactly the same position as that observed in the spectrum of the untreated kaolinite, although the FWHM increased with reaction time. Such behavior indicates that, although the hydrothermal reaction induced a certain degree of disorder in the Si nuclei of kaolinite, the nature of the neighboring atoms of a considerable number of Si nuclei was unchanged, even after 13 and 24 h, while the XRD patterns indicated the formation of real illite/muscovite crystals. Clearly, not

all kaolinite particles are undergoing transformation at the same time; a considerable proportion of the kaolinite remains intact after each treatment, even after 24 h of reaction. The reaction mechanism probably goes through the transformation of the layers from the external surface to the interior of the kaolinite particles, so that untransformed, intact kaolinite layers remain in the inside of the particles while the outer layers have fully transformed into illite/muscovite crystals.

CONCLUSIONS

The illitization of kaolinite in a KOH solution at high solid/liquid ratio takes place through a topotactic replacement which starts with the diffusion of Al from the octahedral to the tetrahedral sheet of the kaolinite TO layers, giving rise to the precursors of the illite/muscovite nuclei. Transformation of those precursors to illite/muscovite nuclei requires condensation of a second tetrahedral sheet, which, in view of the XRD and ^{27}Al MAS NMR measurements, does not take place until a minimum amount of Al has occupied the tetrahedral sheet of the TO structure.

ACKNOWLEDGMENTS

Dr D. Dolejs and Dr H. Keppler are gratefully acknowledged for help with the hydrothermal reactors. This work was carried out with financial assistance by a project funded within the VI Framework Program as an HRM Activity under contract number MRTN-CT-2006-035957, by DGICYT Project no. CTQ2007-63297, and by an Excellence Project of Junta de Andalucía P06-FQM-02179.

REFERENCES

Ahn, J.H. and Buseck, P.R. (1986) Transmission and analytical electron microscopy of the smectite to illite transition. *Clays and Clay Minerals*, **34**, 165–179.

Altaner, S.P. and Ylagan, R.F. (1997) Comparison of structural models of mixed-layer illite/smectite and reaction mechanism of smectite illitization. *Clays and Clay Minerals*, **45**, 517–533.

Bailey, S.W. (1984) Classification and structures of micas. Pp. 1–12 in: *Micas* (S.W. Bailey, editor). Reviews in Mineralogy, **13**, Mineralogical Society of America, Washington, D.C.

Bauer, A. and Berger, G. (1998) Kaolinite and smectite dissolution rate in high molar KOH solutions at 35ºC and 80ºC. *Applied Geochemistry*, **13**, 905–916.

Bauer, A., Velde, B., and Berger, G. (1998) Kaolinite transformation in high molar KOH solutions. *Applied Geochemistry*, **13**, 619–629.

Bentabol, M., Ruiz Cruz, M.D., Huertas, F.J., and Linares, J. (2003a) Hydrothermal transformation of kaolinite to illite at 200 and 300ºC. *Clay Minerals*, **38**, 161–172.

Bentabol, M., Ruiz Cruz, M.D., Huertas, F.J., and Linares, J. (2003b) Characterization of the expandable clays formed from kaolinite at 200ºC. *Clay Minerals*, **38**, 445–458.

Bentabol, M., Ruiz Cruz, M.D., Huertas, F.J., and Linares, J. (2006) Chemical and structural variability of illitic phases formed from kaolinite in hydrothermal conditions. *Applied Clay Science*, **32**, 111–124.

Chermak, J.A. and Rimstidt, J.D. (1990) The hydrothermal transformation rate of kaolinite to muscovite/illite. *Geochimica et Cosmochimica Acta*, **54**, 2979–2990.

De Almeida Martins, L. (1999) Illitisasion des minéraux argileux du groupe kaolin dans le champs pétrolier de Rind (Norvège). DEA Thesis, Université de Poitiers, France.

Dutta, P.K. and Suttner, L.J. (1986) Alluvial sandstone composition and paleoclimate. II. Authigenic mineralogy. *Journal of Sedimentology and Petrology*, **56**, 346–358.

Engelhardt, G. and Michel, D. (1987) *High-Resolution Solid state NMR of Silicates and Zeolites.* John Wiley and Sons, New York, 179 pp.

Grim, R.E. (1968) *Clay Mineralogy.* McGraw-Hill Book Company, New York.

Hancock, N.J. and Taylor, A.M. (1978) Clay mineral diagenesis and oil migration in the Middle Jurassic Brent Sand Formation. *Journal of the Geological Society*, **135**, 69–72.

Huang, W.L. (1993) The formation of illitic clays from kaolinite in KOH solution from 225ºC to 350ºC. *Clays and Clay Minerals*, **41**, 645–654.

Inoue, A. and Utada, M. (1983) Further investigations of a conversion series of dioctahedral mica/smectites in the Shinzan hydrothermal alteration area, northeast Japan. *Clays and Clay Minerals*, **31**, 401–412.

Inoue, A., Velde, B., Meunier, A. and Touchard, G. (1988) Mechanism of illite formation during smectite-to-illite conversion in a hydrothermal system. *American Mineralogist*, **73**, 1325–1334.

Inoue, A., Watanabe, T., Koyhama, N. and Brusewitz, A.M. (1990) Characterization of illitization of smectite in bentonite beds at Kinnekulle, Sweeden. *Clays and Clay Minerals*, **38**, 241–249.

Jennings, S. and Thompson, G.R. (1986) Diagenesis of Plio-Pleistocene sediments of the Colorado River delta, southern California. *Journal of Sedimentary Petrology*, **56**, 89–98.

Kinsey, R.A., Kirkpatrick, R.J., Hower, J., Smith, K.A., and Oldfield, E. (1985) High-resolution Al-27 and Si-29 Nuclear Magnetic-Resonance spectroscopic study of layer silicates, including clay-minerals. *American Mineralogist*, **70**, 537–548.

Kirkpatrick, R.J., Kinsey, R.A., Smith, K.A., Henderson, D.M., and Oldfield, E. (1985) High-resolution solid-state Na-23, Al-27, and Si-29 Nuclear Magnetic-Resonance spectroscopic reconnaissance of alkali and plagioclase feldspars. *American Mineralogist*, **70**, 106–123.

Liebau, F. (1985) *Structural Chemistry of Silicates*. Springer-Verlag, Berlin.

Lipsicas, M., Raythatha, R.H., Pinnavaia, T.J., Johnson, J.D., Giese, R.F., Costanzo, P.M., and Roberts, J.L. (1984) Silicon and Aluminum site distributions in 2-1 layered silicate clays. *Nature*, **309**, 604–605.

Madejová, J. and Komadel, P. (2001) Baseline studies of the Clay Minerals Society source clays: Infrared methods. *Clays and Clay Minerals*, **49**, 410–432.

Martín-Martín, J.D., Gómez-Gras, D., Sanfeliu, T., Permanyer, A., Núñez, J.A., and Parcerisa, D. (2006) Conditions of kaolin illitization in the Permo-Triassic sandstones from the SE Iberian Ranges, Spain. *Journal of Geochemical Exploration*, **89**, 263–266.

Mermut, A.R. and Faz Cano, A. (2001) Baseline Studies of the Clay Minerals Society Source Clays: Chemical analysis of major elements. *Clays and Clay Minerals*, **49**, 381–386.

Pollard, C.O. (1971) Appendix: Semidisplacive mechanism for diagenetic alteration of montmorillonite layers to illite layers. *Geological Society of America, Special Papers*, **134**, 79–93.

Sanz, J. and Serratosa, J.M. (1984) ^{29}Si and ^{27}Al High

Resolution MAS NMR Spectra of Phyllosilicates. *Journal of the American Chemical Society*, **106**, 4790–4793.

Schoonmaker, J., Mackenzie, F.T., and Speed, R.C. (1986) Tectonic implications of illite/smectite diagenesis, Barbados accretionary prism. *Clays and Clay Minerals*, **34**, 465–472.

Sommer, F. (1978) Diagenesis of Jurassic sandstones in the Viking Graben. *Journal of the Geological Society*, **125**, 63–67.

Velde, B. (1965) Experimental determination of muscovite polymorph stabilities: *American Mineralogist*, **50**, 436–449.

Weaver, C.E. and Beck, K.C. (1971) Clay water diagenesis during burial: how much become gneiss. *Geological Society of America, Special Papers*, **134**, 1–96.

Weiss, C.A., Altaner, S.P., and Kirkpatrick, R.J. (1987) High-resolution 29Si NMR spectroscopy of 2:1 layer silicates: Correlations among chemical shift, structural distortions, and chemical variations. *American Mineralogist*, **72**, 935–942.

Woessner, D.E. (1989) Characterization of clay minerals by Al-27 nuclear magnetic resonance spectroscopy. *American Mineralogist*, **74**, 203–215.

Yau, L., Peacor, D.R., and McDowell, S.D. (1987) Smectite to illite reactions in Salton Sea shales: A transmission and analytical electron microscopy study. *Journal of Sedimentary Petrology*, **57**, 335–342.

(*Received 26 August 2008; revised 27 January 2009; Ms. 0194; A.E. W. Jaynes*)